# ARTICLES

## Dynamics of Excited Solvated Electrons in Aqueous Solution Monitored with Femtosecond-Time and Polarization Resolution

**M. Assel, R. Laenen,* and A. Laubereau**

*Physik-Department E 11, Technische Universität München, D-85748 Garching, Germany*

*Received: July 30, 1997; In Final Form: January 20, 1998*

Transient pump−probe spectroscopy of equilibrated solvated electrons is carried out in aqueous NaCl solution (5.9 M) in the visible and near-infrared using pulses of 100−170 fs duration and polarization resolution. Excitation is performed by a pump pulse at 620 nm in the blue wing of the electronic absorption band. Transient bleaching occurs in a broad interval around the maximum of the $e^-$ absorption at 705 nm, accompanied by induced absorption at longer wavelengths. No hole-burning features are observed within our experimental time resolution suggesting a time constant $\tau_1 < 80$ fs for rapid solvent relaxation and/or population redistribution among the excited electronic states. The relaxation dynamics involves a first intermediate, a frequency-shifted excited-state p′ with lifetime $\tau_2 = 190 \pm 40$ fs. A further time constant $\tau_3 = 1.2 \pm 0.4$ ps accounts for the recovery of the ground state. The latter process involves a second intermediate that is assigned as a modified ground-state s″. Evidence for stimulated emission suggests a distinct red shift of the transition p′→ ground state to 800 ± 20 nm, while the transient absorption band of electrons in the s″-level is centered at 780 ± 20 nm. The negligible anisotropy <0.01 of the probe absorption measured during and after the excitation process indicates that the observed distribution of solvent cavities of hydrated electrons is close to spherical symmetry.

### 1. Introduction

The solvated electron was extensively studied during the past decades. It appears as one of the first reaction steps in a number of chemical and photochemical reactions and may also serve as a fast spectral probe for the dynamics of the solvent surroundings. Especially the solvated electron in water was of great interest in recent years owing to the abundance of the liquid in biological systems. The simple structure of a single electron captured in a solvent cavity makes it predestinate to quantum molecular dynamics calculations.

First results on its optical properties were reported in the early sixties, when a broad structureless absorption band centered at 720 nm was found in radiolysis studies.[1] The same absorption spectrum appears after optical excitation of neat water by an intense laser pulse in the UV region.[2] In fact, via two- and three-photon absorption at 310 nm[3−6] or 390 nm[7] and even higher-order multiphoton absorption in the visible at 620 nm,[8] the solvated electron can be produced. The two-photon excitation mechanism was verified very recently for femtosecond pulses at 282 nm (8.8 eV).[9] The quantum yield of electron formation by photoionization of water molecules was determined to be 0.11 ± 0.03 per absorbed photon. A brief review of different ways to generate the solvated electron by laser irradiation is presented in refs 10, 11.

The proposed structure of the hydrated electron is the following: the electron is trapped in a solvent cavity formed by six water molecules[12,13] with a radius of 2.1−2.2 Å.[12] An elliptical shape of the cavity was deduced from computer simulations very recently.[14] Details of the structure are still subject to discussion, for example, if the electron is attached more closely to one of the "dangling protons" that are not involved in the hydrogen bonding of the molecules forming the solvent cage.[15] The ground level of the electron in this cavity is an s-like eigenstate, and the absorption band centered at 720 nm represents a predicted 1s→ 2p transition with possible substructure due to three substates separated by approximately 0.5 eV.[16] Further excited levels that are believed to be continuum states are positioned roughly 1 eV above the 2p-level. These levels should be interpreted as dressed states of the electron coupled to the almost instantaneously responding electronic polarization of the surrounding solvent molecules giving rise to a distinct renormalization of the energy levels.[17]

The femtosecond photoionization of water is followed by a transient absorption spectrum located in the near-infrared (NIR) region. It appears with a rise time of 110−180 fs[3−5,7,9] which could be attributed to a precursor of the solvated electron, the wet electron. The detailed character of the intermediate is still under investigation. The decay of the primary absorption band occurs on a subpicosecond time scale (≃540 ± 50 fs)[4,9] and is accompanied by the buildup of the absorption band of the solvated electron at 720 nm. In addition, but on a slower (picosecond) time scale, geminate recombination of the solvated electrons takes place.[6,9,11,18] The probability to escape the latter process amounts to 0.45−0.7, depending on excitation energy.

Compared to neat water, aqueous solutions of halide salts display larger yields of solvated electrons for given excitation conditions. Halide solutions show an absorption at wavelengths <300 nm that is not observed in the crystalline state and is

S1089-5639(97)02499-7 CCC: $15.00 
Published on Web 03/06/1998

termed the charge-transfer-to-solvent band (CTTS). Absorption into this band results in the ejection of an electron that is rapidly captured and solvated. A small blue shift and narrowing of the absorption band of the equilibrated solvated electron is noticed in the halide solutions,[18−21] which is explained by the additional attractive Coulomb potential between the solvated electron and the cations. The temporal behavior of the aqueous solution after UV excitation was experimentally and theoretically studied in refs 18, 22−24 and 25−28, respectively.

The lifetime of the solvated electron is in general longer than several nanoseconds depending on the concentration of electron scavengers in the water. Other photoproducts, especially the excited anions, absorb in different spectral regions.[29] For this reason it is possible to perform pump−probe spectroscopy of the long-lived, thermalized solvated electron several nanoseconds after its formation. An experiment of this kind was carried out by Barbara and co-workers with pump pulses at 780 nm, 0.15 eV below the maximum of the absorption band.[30,33,34] The dynamics of the excited solvated electron was found to be governed by two time constants with combined bleaching and induced absorption in the spectral region around 800 nm. The complex behavior could not be described by a simple two-level model. Heating[30] or reorientational relaxation of the solvent environment of the trapped electron[14,16] in combination with radiationless decay from the excited state to the s-ground state are considered as possible explanations of the complex absorption transients.

In this paper we present experimental data for the solvated electron with excitation at 620 nm into the blue wing of the quasi-stationary absorption band. The chosen excitation condition may provide information on the structure of the excited energy levels of the trapped electrons, for example, the substructure of the 2p-state. Working at 620 nm, we also avoided unwanted modifications of the highly interesting 800-nm region by a pump−probe coupling artifact. Our polarization-dependent measurements of the transient absorbance changes shed new light on the question of anisotropy and orientational motion of the solvent cavity.

## 2. Experimental Section

The measurements are performed with a colliding pulse mode-locked (CPM) dye laser system. The laser oscillator produces 100-fs pulses with an energy of 200 pJ centered at a wavelength of 620 nm. Single pulses are amplified in a six-pass preamplifier[31] followed by a single pass through a transversally pumped dye amplifier stage.[32] The pulse energy amounts to 30 $\mu$J for a repetition rate of 50 Hz. Compression of the amplified pulses in a two-prism setup restores the initial pulse duration of 100 fs. To study the relaxation dynamics of the equilibrated solvated electron, three laser pulses are required at different wavelengths.[30,33,34] First, an intense pulse in the UV is needed to produce the solvated electrons via multiphoton absorption of water and of dissolved anions. The UV preparation pulse is derived from second-harmonic generation of the amplified CPM pulse in a 2-mm KDP crystal. Energy conversion of up to 20% leads to pulse energies of 6 $\mu$J at 310-nm wavelength and 220-fs pulse duration. The pump−probe experiment is performed 1 ns after the generation process. The nanosecond delay allows for the thermalization of the solvated electrons. One fraction of the laser pulse at 620 nm serves for the excitation of the equilibrated electrons. The probing pulses are derived from the remainder of the laser pulse by supercontinuum generation in a fused silica plate (thickness 5 mm). The useful wavelength range of the probe continuum extends from 550 nm to 1.1 $\mu$m with a measured pulse duration of 170 ± 20 fs.

The three incident beams are focused with linear polarizations into the sample cell using separate polarizers and lenses. The polarization plane of the input probe is set at an angle of 45° relative to the pump. Suitable detectors monitor the input energies of the UV preparation pulse and of the 620-nm pump pulse. The probing beam behind the sample is directed through a small grating spectrometer followed by a polarizer and two detectors measuring the parallel and perpendicular components of the transmitted probe signal. Shot-to-shot energy fluctuations of the incident probe radiation are monitored by the help of a reference beam that is coupled out by a broad-band beam splitter in front of the sample and passes through the same spectrometer for subsequent detection. In this way both polarization components of the energy transmission of the sample, $T_{\parallel}$ and $T_{\perp}$, are simultaneously measured for the wavelength setting of the spectrometer, providing also information on the induced optical anisotropy. The anisotropy $R$ used in the following is defined as

$$R(t_D) = \frac{T_{\parallel} - T_{\perp}}{T_{\parallel} + 2T_{\perp}}$$

where $t_D$ denotes the delay time between pump and probe radiation. It was verified experimentally that cross-talk between the two polarization channels of the probe measurement, $\parallel$ and $\perp$, by imperfections of the optical components is negligible. The spectrometer serves as a spectral filter of the probe continuum selecting radiation with 5-nm bandwidth at the variable-wavelength positions. Transient probe spectra are obtained in consecutive measurements tuning the spectrometer.

The sample cell of 250-$\mu$m thickness is equipped with 1-mm $CaF_2$ windows to minimize a nonlinear signal contribution of the window material. The sample is an aqueous NaCl solution prepared from tridistilled water with a concentration of sodium chloride (Aldrich 99+%) of 5.9 M. Adjusting this salt concentration in the sample results in an increase of the solvated electron yield of a factor of about 10 in comparison to neat water. To avoid accumulative thermal effects the excitation volume is replaced between two consecutive laser pulses by a lateral motion of the sample cell. All measurements are performed at room temperature.

An experimental artifact relevant especially for the measurement of the induced anisotropy of the sample is depicted in Figure 1a,b. The pump−probe experiment is carried out without the UV preparation pulse; i.e., the transient response of the sample cell is measured in the absence of solvated electrons. The induced absorption data for probing at 760 nm are plotted in Figure 1a for parallel and perpendicular polarizations (full points and open circles, respectively). A coherent interaction between pump and probing radiation is observed that may be explained by impulsive stimulated Raman scattering in the cell windows and sample.[35−37] The contribution of the coherent feature to the overall parallel signal ranges between 10% and 50%, depending on the wavelength. The resulting induced anisotropy $R$ is depicted in Figure 1b as a function of delay time. Similar findings are made at other probing wavelengths (UV preparation blocked). We have measured this coherent coupling signal at each investigated spectral position with blocked UV pulse and corrected subsequently all pump−probe data of the solvated electrons for this feature (see below) in order to obtain the pure dynamics of the solvated electron. The

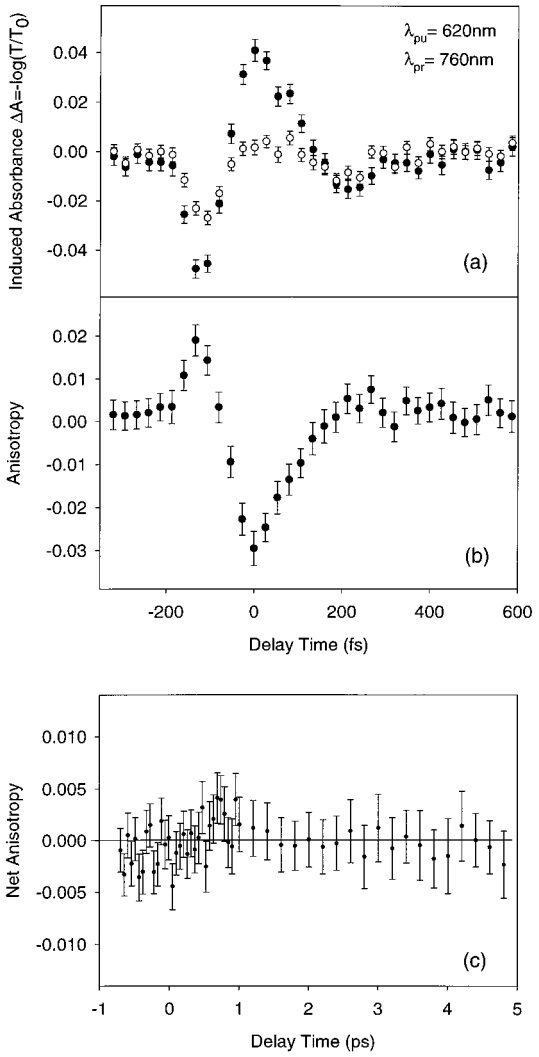


**Figure 1.** (a) Induced absorption of the sample cell without solvated electrons (UV preparation pulse blocked) plotted versus delay time between 620-nm pump and 760-nm probing pulses for parallel (filled circles) and perpendicular probe polarization (hollow circles). (b) Same data as in (a) plotting the induced optical anisotropy $R$; a coherent pump−probe artifact is observed. (c) Net contribution of the solvated electrons to the measured induced optical anisotropy of the sample cell at 760 nm after correction of the artifact of (b); experimental points.

measurements without UV preparation pulse also provide an accurate determination of the zero setting of the delay time scale at the varying wavelength settings; $t_D = 0$ ps occurs close to the maximum of the coherent coupling transient[38] as substantiated by a careful calibration technique. To this end, the zero delay time was deduced from transient absorption measurements of suitable dye solutions in the same pump−probe geometry and comparison with model calculations. The accuracy of the zero setting of our delay time scales is estimated to be ±50 fs.

## 3. Results

Some data on the well-known absorption of the equilibrated $e^-_{solv}$ in water are presented in Figure 2a. The results of ref 39 are plotted versus photon energy (full squares). In an attempt to support the theoretical predictions on the substructure of the p-state,[16] the broad absorption band centered at ≈1.72 eV of the electrons in the s-ground state[39] is deconvolved into three peaks; for the sake of simplicity a Gaussian band shape and equal bandwidths are assumed for the three subcomponents (dashed curves) termed $p_1$ to $p_3$.[40] Fitting the calculated total

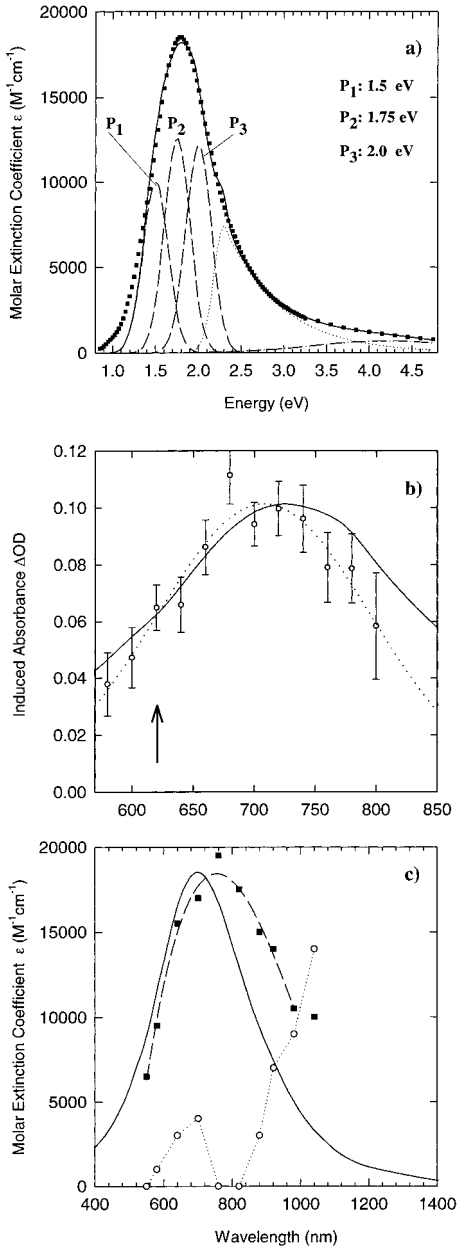


**Figure 2.** (a) Quasi-stationary absorption spectrum of the solvated electron in neat water in the 1s-ground state; experimental points taken from ref 39; the band is tentatively decomposed in three lines $p_1$ to $p_3$ of assumed Gaussian shape and additional absorption by transitions to c-states; calculated curves. (b) Measured 1s-absorption band of thermalized solvated electrons in a 5.9 M aqueous NaCl solution, measured 1 ns after the UV generation process with the femtosecond probing continuum (pump pulse blocked); experimental points and broken line; band center at 705 nm; solid curve: corresponding absorption in neat water centered at 720 nm after ref 41; vertical arrow marks the position of excitation. (c) Probe absorption coefficients used for the fitting of the calculated curves for the model of Figure 5 to the transient data of Figures 3 and 4. 1s-absorption: solid line (data taken from Figure 2b). s″-absorption: filled squares, broken experimental curve. p′-absorption: hollow circles, dotted experimental line; see text.

absorption (solid line) to the experimental data in the region 1.2−2.3 eV suggests line positions of 1.5 eV (827 nm), 1.75 eV (709 nm), and 2.0 eV (620 nm). For the bandwidth of the individual subcomponents a value of ≈0.35 eV (fwhm) is inferred. These numbers, although of semiquantitative character only, agree amazingly well with theoretical predictions.[16] A more accurate fit, for example, using Voigt profiles and different bandwidths, is not attempted. The absorption for higher

energies, >2.3 eV, may be assigned to transitions to predicted continuum states (dotted line). These levels will be referred to as c-states in the following. The estimated position of the $s-p_3$ transition (see Figure 2a) is close to our pumping wavelength of 620 nm. Our tentative band analysis suggests that a higher electronic level and not the first excited state is primarily populated in our pump−probe measurements. Important advantages of this approach compared to longer pumping wavelengths are that information on population redistribution among the p-states may be provided and that the significant spectral dynamics around 800 nm is not perturbed by a coherent pump−probe artifact.

Some experimental data on the absorption of the solvated electron in the thermalized 1s-ground state under our experimental conditions are shown in Figure 2b. The absorption change of the sample is monitored 1 ns after the UV preparation pulse with the white-light continuum (pump pulse at 620 nm blocked) and plotted in the figure versus probing wavelength (experimental points, dashed curve). Apart from a minor blue shift of 15 ± 8 nm (37 meV), the measured absorption in the NaCl solution is very similar to the reported absorption band of the solvated electron in neat water (solid line).[41] The spectral shift is in qualitative agreement with findings for other electrolytes.[19] The mean distance of the Cl atom to the $e^-$ is estimated to be approximately 6 Å, for times greater than 2 ps after the UV preparation pulse.[25] On the other hand, the distance between the $e^-$ and the nearest hydrogen atoms of the surrounding water molecules was calculated to be in the range of 2.1−2.8 Å[42] and measured to be 2.1 ± 0.1 Å.[12] The numbers indicate that electrons escaping geminate recombination are mainly surrounded in the first solvation shell by water molecules, even at the NaCl concentration used in this investigation. It may be surmised that the dynamics of thermalized solvated electrons studied here in solution should be directly comparable to data for neat water.

In Figure 3 we present results of our time-resolved absorption measurements at various probing wavelengths. The filled and hollow circles represent the experimental data for parallel and perpendicular polarization of the probe, respectively. The solid lines in the figure are obtained from model calculations described in the following section. All measurements are performed for constant amplitudes of the UV preparation and 620-nm pump pulses. Therefore, the amplitudes of the absorbance changes at the different wavelengths are directly comparable to each other. For probing at wavelengths shorter than 700 nm, the transients show a very similar behavior. Around $t_D = 0$ ps a fast decrease of the absorption of the sample is observed within the time resolution of the experimental system and attributed to a depletion of the s-ground state and population of the excited states of the electrons. This bleaching subsequently decays, at first rapidly and later on more slowly. For delay times longer than 3 ps, the absorption has almost returned to its initial value. The differences between the calculated curves and the measured data points are due to the slight scatter at late delay times not significant enough to be taken into account for further considerations. A more complex behavior is found in the wavelength range 760−1040 nm. The initial bleaching of the sample is less pronounced than for shorter wavelengths and rapidly followed by an induced absorption that in turn vanishes almost completely with a relaxation time close to 1 ps. Above 920 nm (not shown; see curves for 980 and 1040 nm), the bleaching component has disappeared and only a delayed onset of induced absorption is observed, which recovers monotonically. The maximum amplitudes of the initial

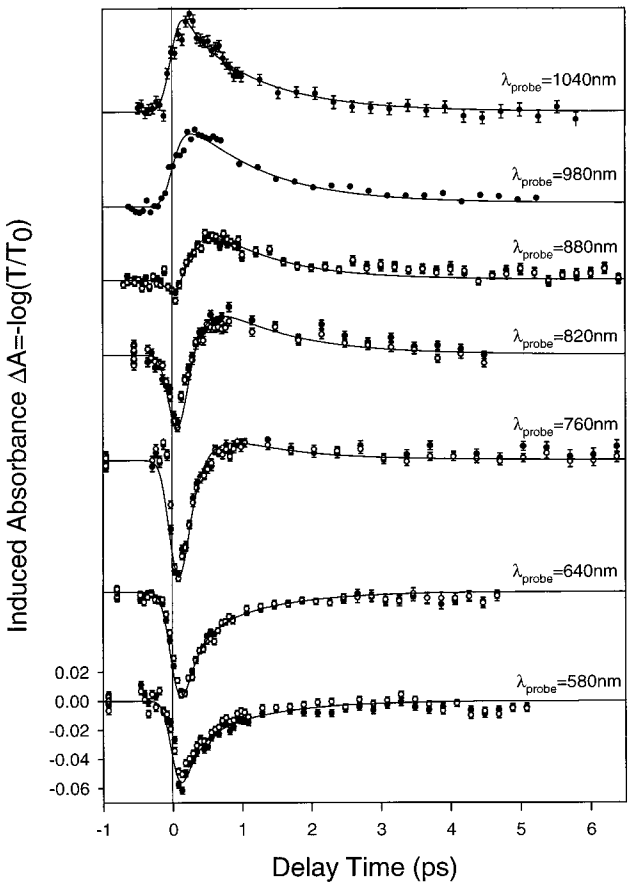


**Figure 3.** Measured transient absorption changes of solvated electrons in aqueous NaCl solution versus delay time in the wavelength range 580−1040 nm after excitation at 620 nm for parallel (filled circles) and perpendicular probe polarization (hollow circles); fitted calculated curves using the model of Figure 5. The zero delay settings for the various wavelengths are determined in independent measurements (±50 fs); see text.

bleaching ($t_D \approx 130$ fs) and of the induced absorption ($t_D \approx 500$ fs) occur at probing wavelengths of 760 and 920 nm, respectively, with an amplitude ratio of approximately 2. At a probing wavelength of 760 nm, we have reduced the estimated pump intensity of ≈4 GW/cm$^2$ by a factor of 4 in order to investigate the intensity dependence of the excitation process (data not shown). Within our accuracy we found only the expected decrease of the signal amplitude and no differences in the measured dynamics indicating a minor contribution of two-step excitation of the solvated electron to the continuum.

The data of Figure 3 are corrected for the coherent coupling artifact of the sample cell discussed in the context of Figure 1. The polarization dependence of the signal transients completely disappears after correction for the artifact. An example is shown in Figure 1c for probing at 760 nm. The contribution of the solvated electrons to the measured optical anisotropy of the sample is plotted versus delay time and found to be negligible within our experimental accuracy. The same finding holds for all other probing wavelengths, i.e., $|R| < 0.01$.

Corresponding transient absorption spectra are depicted in Figure 4 for several delay time values (experimental points). The position of the excitation pulse at 620 nm is marked by a vertical arrow. It is interesting to see that the maximum bleaching does not occur at 705 nm as expected for the equilibrium s−p absorption (see Figure 2) but is red shifted to approximately 760 nm with a remarkedly extended wing into the visible, considerably broader than the quasi-stationary

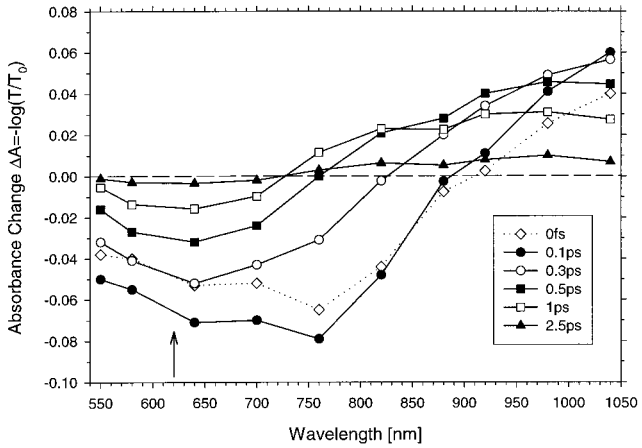


**Figure 4.** Transient absorption spectra of the solvated electrons in the aqueous NaCl solution (5.9 M) in the range 550−1040 nm for various delay times listed in the inset; experimental points. Lines are drawn as guides to the eye. The position of the pump pulse is marked by a vertical arrow; the dashed line indicates zero absorbance change.

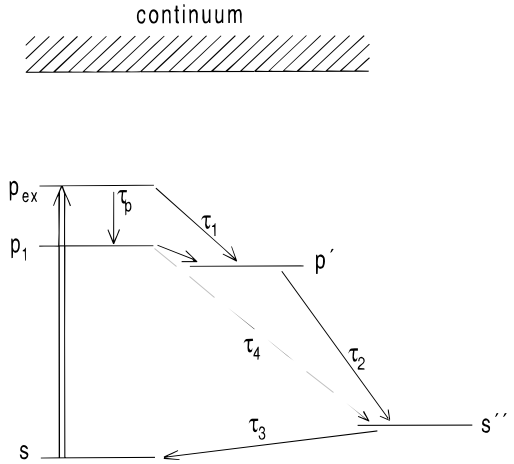


**Figure 5.** Simplified energy-level scheme used to describe the relaxation dynamics of the solvated electron in aqueous solution with intermediate levels p′ and s″ involving spectral relaxation of the solvent cage. The double arrow represents the pumping process; arrows indicate population transfer processes. For discussion, see text.

absorption band. No evidence for spectral hole burning is found below 700 nm within the time resolution of our measurement. The broad bleaching feature indicates that for wavelengths below ≈730 nm the ground-state depletion dominates excited-state absorption (ESA). A different temporal behavior is found at longer wavelengths, where induced absorption occurs. Owing to the smaller transition energy from p- to c-states (≤1 eV), as compared to the s−p band (1.76 eV), ESA is expected to dominate for sufficiently long wavelengths in the NIR. The absence of an isosbestic point in the range 700−900 nm directly indicates that a two-level approach cannot account for the observed dynamics.

## 4. Discussion

The signal transients presented in Figure 3 are in accordance with the measurements of Barbara and co-workers.[30] These authors explain the complex behavior of the absorption transients by solvent relaxation and local heating during the rapid internal conversion of the excited $e^-$ state to a modified, longer-lived ground state. Our interpretation is somewhat different in detail and supported in part by several theoretical investigations.[14,16,28,43] These authors emphasize fast solvent reorganization around the excited electrons in the p-state followed by internal conversion. For a qualitative understanding of our data, several basic features should be emphasized first:

(i) There is no indication in Figure 4 for spectral hole burning around the pump wavelength (620 nm); because of the large spectral bandwidth, such a phenomenon may extend in the wings until 550 and 700 nm, respectively. It is concluded that rapid population transfer occurs to the first excited electronic level ($p_1$ in Figure 2a) and/or fast spectral relaxation of the s−p transition on a sub-100-fs scale.

(ii) The maximum bleaching at zero delay and $t_D = 100$ fs is observed at 760 nm, notably red shifted compared to the band maximum (705 nm) of the equilibrated electrons. The phenomenon occurs despite the onset of excited-state absorption at longer wavelengths and presents again evidence for rapid population redistribution to a lower-lying excited state and/or spectral relaxation of the s−p transition in combination with stimulated emission. Since the broadest bleaching interval already shows up at zero delay time, these processes again appear comparable to or faster than the experimental time resolution.

(iii) Despite the red shift of the fundamental transition, excited-state absorption dominates in the NIR. During the first 100 fs, it starts at approximately 900 nm, and from the steep slope at 1 $\mu$m, it may be guessed that it extends considerably in the IR ($t_D = 100$ fs). For later times the induced absorption expands to shorter wavelengths within a few hundred femtoseconds. The finding may be explained by internal conversion to a modified ground state s″ with red-shifted absorption. Comparison of the transient absorption curves for 500 fs and 1 ps shows that the dynamics has already slowed considerably in this time interval, suggesting a time constant $\tau_2 < 500$ fs for the population decay time from an intermediate level that will be termed p′ in the following to the modified ground state s″.

(iv) For longer times, $t_D > 1$ ps, the zero crossing of the transient absorption curves remains constant. It is proposed that the internal conversion process of the excited electrons now has terminated and that the small remaining dynamics (see Figure 4) may represent a slow thermalization process of the electrons in the modified s″-state returning to the original s-ground level and/or further rearrangement of the solvent layer. The induced absorption in the NIR now can be solely explained by the red shift of the s″-absorption compared to the quasi-equilibrium s-band.

For a more quantitative analysis, the physical picture is cast into a five-level scheme for the solvated electrons that is depicted in Figure 5. Our simplified model can reproduce the essential physical features of the observed relaxation dynamics. Starting from the s-state, about 50% of the thermalized solvated electrons are excited by the 620-nm pump pulse and promoted to a higher excited p-state, termed the $p_{ex}$-level. The primary excess population there decays with time constant $\tau_p$ to the lowest excited state $p_1$. Simultaneously a certain rearrangement of the solvent layer sets in. According to theoretical data[14] the solvent reorganization involves two time scales: a fast Gaussian component with approximately 25 fs and a slower exponential contribution with 250 fs. Similar, but quantitatively different, data were already reported from ref 16. The dynamical solvent shift is explicitly considered in the model of Figure 5 by the relaxation time $\tau_1$ for the population of a modified electronic state p′. The former fast process with Gaussian time dependence is not accessible with our time resolution and not explicitly considered, but contained to some extent in the redistribution process of the p-states with time $\tau_p$. The population of p′ decays

to a modified ground state s″ (denoted in the figure by one energy level for simplification) with time constant $\tau_2$ that is predicted to be 730 fs.[16] Final relaxation to the initial solvent structure is described in Figure 5 by a time constant $\tau_3$ for the recovery of the original ground state 1s.

It is not clear a priori if solvent relaxation and internal conversion of the electronic excitation are sequential processes because of considerably different relaxation rates or proceed simultaneously on comparable time scales. To include a parallel decay channel, a direct transfer rate from $p_1$ to s″ with time constant $\tau_4$ is also considered. The terminal states of probing transitions starting from p′- or s″-levels are not indicated in Figure 5 and need not be specified for the population dynamics (see below). Besides p′ that is introduced as the modified first excited electronic state, other excited levels with relaxed solvent configurations are expected to exist but are not considered for the measured relaxation dynamics.

The solid lines in Figure 3 are calculated from rate equations according to the five-level model of Figure 5 and fitted to the time-dependent experimental data for one set of time constants. The nonobservation of spectral hole burning provides an upper limit of $\tau_p < 80$ fs for the redistribution time of the p-states. Our analysis also strongly suggests that the relaxation of the solvent cage represented by time constant $\tau_1$ is fast compared to experimental time resolution, i.e., $\tau_1 < 80$ fs. A moderately fast component of spectral relaxation with time constant of a few hundred femtoseconds is not seen. The lifetime of the first intermediate p′ is determined to be $\tau_2 = 190 \pm 40$ fs. The lifetime of the second intermediate s″ relevant for the ground-state recovery is found to be $\tau_3 = 1.2 \pm 0.4$ ps. Direct conversion from the excited p-level ($p_{ex}$, $p_1$) to the modified s′-ground state as described by time constant $\tau_4$ is found to be negligible ($\tau_4 > 400$ fs). In other words, there is clear evidence for a first intermediate with lifetime 190 fs that is spectrally different to the primary excitation of the pump pulse.

The probe absorption cross sections of the s″- and p′-levels in the range 550−1040 nm were used as adjustable parameters in the fitting process. The results are depicted in Figure 2c and allow one to check the self-consistency of the model. For the s-absorption (full line) of electrons remaining in the ground state, the quasi-stationary band (Figure 2b) that is positioned at 705 nm for our NaCl solution is used. The absorption of the relatively long-lived intermediate s″ is uniquely determined from the dynamics for $t_D > 1$ ps and represented by filled squares in the figure (dashed curve). It is interesting to notice the band position at approximately 780 nm, red shifted by $170 \pm 50$ meV, and the bandwidth of $920 \pm 50$ meV close to the width of the s-absorption. The result for the transient s″-band strongly supports the assignment of this level as a modified ground state.

The transient probe absorption of electrons in the p′-level deduced from the measured subpicosecond dynamics is indicated in Figure 2c by open circles (experimental dotted curve). The cross section curve is seen to increase from 600 to 1000 nm (2.1−1.2 eV) with a distinct gap around 800 nm. Tentatively, we separate the excited-state absorption of p′ by a comparison with the c-absorption in Figure 2a) above 2.5 eV, suggesting a monotonic increase. The amplitude difference to the experimental points (hollow circles) around 800 nm is particularly interesting and explained by stimulated emission from the p′-state to a corresponding ground state, tentatively assigned as s′-level (presumably not identical to s″). The stimulated emission feature noticed here represents a necessary consequence of our theoretical model, since the transient population of an intermediate state p′ with 190-fs lifetime involves population inversion. The finding provides evidence that

the first measurable intermediate p′ with lifetime 190 fs represents an excited electronic state;

the position of energy level p′ is close to p within a few hundred millielectronvolts;

the p′−s′ transition positioned at $800 \pm 20$ nm differs from the s″-absorption.

The role of solvent relaxation for the spectral shift of the p′−s′ transition remains unclear, since the levels $p_1$ and p′ cannot be distinguished within our experimental time resolution and measuring accuracy. In other words, the red shift in the stimulated emission band may be explained to a large extent by the energy difference of the first excited state $p_1$ as compared to the maximum of the equilibrium s-absorption. The results of Figure 2c give considerable support to the physical picture of Figure 5. The excited-state absorption of the short-lived $p_{ex}$- and $p_1$-levels cannot be inferred from the probe spectra because of the fast transit to p′. As a zero-order approximation the same cross sections as for p′ were used for these minor level populations that are negligible for $t_D = 100$ fs and later times; i.e., the simplifying assumption is numerically insignificant. The red shift of 170 meV of the s″-absorption may be related to the local temperature increase of the solvated electron that originates from the conversion of the electronic excitation energy to other degrees of freedom (of solvent molecules). From the reported temperature and pressure dependence of the quasi-stationary s-absorption band,[45] the observed spectral shift can be estimated to be consistent with a temperature increase of the solvent cage of approximately 90 K, a reasonable value; the underlying assumption of quasi-equilibrium in the solvent layer, however, is debatable for the time scale of a few picoseconds. The temperature change induced by the deposited energy in the excited volume is estimated to about 70 K giving support to the number derived from the spectral shift of the respective absorption.

**TABLE 1: Predicted and Measured Relaxation Times of the Solvated Electrons**

| | theory | Barbara and co-workers[a] | this work |
|---|---|---|---|
| $\tau_1$ (fs) | 25,[b] 17[c] | | <80 |
| $\tau_2$ (fs) | 250,[b] 730[c] | 310 ± 80 | 190 ± 40 |
| $\tau_3$ (fs) | | 1100 ± 200 | 1200 ± 400 |

[a] Aqueous solution of KI (50 mM).[30] [b] Neat water.[46] [c] Neat water.[16]

Table 1 summarizes the relaxation times determined in the different investigations. Some of the theoretical predictions are not supported by the present experimental data. The slower component of the solvent cage dynamics (250 fs) is not seen in our investigation. Internal conversion from the excited electronic level to a modified ground state appears to be faster than that derived from simulations. The numbers determined in our investigation are in satisfactory accordance with the results of Barbara's group.[30] The physical picture used by those authors was a three-level model and internal conversion from 2p to a modified ground state. The results of our polarization-dependent measurements differ from previous experimental and theoretical work. Barbara and co-workers[34] reported an anisotropy of approximately 0.05 at several wavelengths with a decay time of 2−3 ps, and Rossky and co-workers[28] predicted an anisotropy with a relaxation time in the range of hundreds of femtoseconds to a few picoseconds, quite different from the simulations of Bratos et al.[16] without induced anisotropy. As pointed out above, we do not see a detectable anisotropy in the wavelength

range 550−1040 nm at the higher electrolyte concentration studied here. Obviously the optical anisotropy disappears at room temperature in time intervals shorter than 80 fs, consistent with the fast relaxation in the excited electronic state, below our experimental time resolution.

## 5. Conclusions

We have investigated the equilibrated solvated electron in an aqueous NaCl solution after excitation into a higher-lying level at 2 eV. The observed relaxation dynamics involves two intermediate states with time constants of 190 fs and 1.2 ps, respectively, that are in satisfactory agreement with previous results for somewhat different experimental conditions as reported by Barbara and co-workers. Our data show that the first intermediate p′ is not the primarily populated excited state of the pumping process ($p_{ex}$ in our theoretical model), but spectrally red shifted to approximately 800 nm. The absence of spectral hole burning and optical anisotropy indicates a fast redistribution of the electronic excitation. The role of solvent relaxation for the energy position of p′, however, remains unclear, since the latter effect cannot be distinguished in the present study from population decay to the first excited electronic level ($p_1$ in our model). Obviously solvent relaxation gives rise to small spectral shifts, only, in the 100 meV range. The second intermediate s″ is a modified electronic ground state. It is clearly red shifted in the spectrum compared to the quasi-equilibrium absorption because of solvent reorganization. The details of the latter process are not fully understood at the present time, although simple heating of the solvent cage is consistent with the observed spectral shift.

**Acknowledgment.** The authors gratefully acknowledge stimulating discussions with Prof. S. Bratos and Dr. A. Staib and the availability of their data prior to publication. They are also indebted to Prof. S. F. Fischer for fruitful comments about the solvation dynamics of electrons.

## References and Notes

(1) Hart, E. J.; Boag, J. W. *J. Am. Chem. Soc.* **1962**, *84*, 4090.
(2) Wiesenfeld, J. M.; Ippen, E. P. *Chem. Phys. Lett.* **1980**, *73*, 47.
(3) Migus, A.; Gauduel, Y.; Martin, J. L.; Antonetti, A. *Phys. Rev. Lett.* **1987**, *58*, 1559.
(4) Long, F. H.; Lu, H.; Eisenthal, K. B. *Phys. Rev. Lett.* **1990**, *64*, 1469.
(5) Shi, X.; Long, F. H.; Lu, H.; Eisenthal, K. B. *J. Phys. Chem.* **1996**, *100*, 11903.
(6) Long, F. H.; Lu, H.; Shi, X.; Eisenthal, K. B. *Chem. Phys. Lett.* **1991**, *185*, 47.
(7) McGowen, J. L.; Ajo, H. M.; Zhang, J. Z.; Schwartz, B. J. *Chem. Phys. Lett.* **1994**, *231*, 504.
(8) Pepin, C.; Houde, D.; Remita, H.; Goulet, T.; Jay-Gerin, J. P. *Phys. Rev. Lett.* **1992**, *69*, 3389.
(9) Reuther, A.; Laubereau, A.; Nikogosyan, D. N. *J. Phys. Chem.* **1996**, *100*, 16794.
(10) Crowell, R. A.; Bartels, D. M. *J. Phys. Chem.* **1996**, *100*, 17940.
(11) Sander, M. U.; Luther, K.; Troe, J. *Ber. Bunsen-Ges. Phys. Chem.* **1993**, *97*, 953.
(12) Kevan, L. *Acc. Chem. Res.* **1981**, *14*, 138.
(13) Reed, A. E.; Clark, T. *Faraday Discuss. Chem. Soc.* **1988**, *85*, 365.
(14) Schwartz, B. J.; Rossky, P. J. *J. Phys. Chem.* **1994**, *98*, 4489.
(15) Kim, K. S.; Park, I.; Lee, S.; Cho, K.; Lee, J. Y.; Kim, J.; Joannopoulos, J. D. *Phys. Rev. Lett.* **1996**, *76*, 956.
(16) Bratos, S.; Leicknam, J.-Cl. *Chem. Phys. Lett.* **1996**, *261*, 117.
(17) Borgis, D.; Staib, A. *Chem. Phys. Lett.* **1994**, *230*, 405.
(18) Gauduel, Y.; Pommeret, S.; Antonetti, A. *J. Phys. IV* **1991**, *1*, C5−127.
(19) Kreitus, I. V.; Strode, D. A. *High Energy Chem.* **1989**, *23*, 172.
(20) Kreitus, I. V. *J. Phys. Chem. 1985*, *89*, 1987.
(21) Lakhno, V. D.; Vasilev, O. V. *Chem. Phys. Lett.* **1991**, *177*, 59.
(22) Gauduel, Y.; Gelabert, H.; Ashokkumar, M. *J. Mol. Liq.* **1995**, *64*, 57.
(23) Gauduel, Y.; Gelabert, H.; Ashokkumar, M. *Chem. Phys.* **1995**, *197*, 167.
(24) Long, F. H.; Shi, X.; Lu, H.; Eisenthal, K. B. *J. Phys. Chem.* **1994**, *98*, 7252.
(25) Staib, A.; Borgis, D. *J. Chem. Phys.* **1996**, *104*, 9027.
(26) Borgis, D.; Staib, A. *J. Phys.: Condens. Matter* **1996**, *8*, 9389.
(27) Borgis, D.; Staib, A. *J. Chem. Phys.* **1996**, *104*, 4776.
(28) Sheu, W.-S.; Rossky, P. J. *J. Phys. Chem.* **1996**, *100*, 1295.
(29) Iwata, A.; Nakashima, N.; Izawa, Y.; Yamanaka, C. *Anal. Sci.* **1993**, *9*, 801.
(30) Kimura, Y.; Alfano, J. C.; Walhout, P. K.; Barbara, P. F. *J. Phys. Chem.* **1994** *98*, 3450.
(31) Knox, W.; Downer, M.; Fork, R. L.; Shank, C. V. *Opt. Lett.* **1984**, *9*, 552.
(32) Bethune, D. S. *Appl. Opt.* **1981**, *20*, 1897.
(33) Alfano, J. C.; Walhout, P. K.; Kimura, Y.; Barbara, P. F. *J. Chem. Phys.* **1993**, *98*, 953.
(34) Reid, P. J.; Silva, C.; Walhout, P. K.; Barbara, P. F. *Chem. Phys. Lett.* **1994**, *228*, 658.
(35) Yan, Y. X.; Gamble, E. B.; Nelson, K. A. *J. Phys. Chem.* **1985**, *97*, 5391.
(36) Yan, Y. X.; Nelson, K. A. *J. Chem. Phys.* **1987**, *87*, 6240.
(37) Vöhringer, P.; Scherer, N. F. *J. Phys. Chem.* **1995**, *99*, 2684.
(38) Kovalenko, S. A.; Ernsting, N. P.; Ruthmann, J. *Chem. Phys. Lett.* **1996**, *258*, 445.
(39) Jou, F.-Y.; Freeman, G. R. *J. Phys. Chem.* **1979**, *83*, 2383.
(40) Abramczyk, H. *J. Phys. Chem.* **1991**, *95*, 6149.
(41) Gauduel, Y.; Martin, J.; Migus, A.; Yamada, N.; Antonetti, A. *Proceedings of the Fifth OSA Topical Meeting, Ultrafast Phenomena V*; Springer Series in Optical Science; Springer: Berlin, Heidelberg, 1986; p 308.
(42) Clark, T.; Illing, G. *J. Am. Chem. Soc.* **1987**, *109*, 1013.
(43) Bratos, S.; Leicknam, J.-Cl.; Borgis, D.; Staib, A. *Phys. Rev. E*, in press.
(44) Rossky, P. J.; Simon, J. D. *Nature* **1994**, *370*, 263.
(45) Jou, F.-Y.; Freeman, G. R. *J. Phys. Chem.* **1977**, *81*, 909.
(46) Schwartz, B. J.; Rossky, P. J. *J. Chem. Phys.* **1994**, *101*, 6902.
(47) Schwartz, B. J.; Rossky, P. J. *Phys. Rev. Lett.* **1994**, *72*, 3282.